3D CHARACTERISATION OF THE TENSILE FAILURE OF CFRPs MANUFACTURED THROUGH TAILORED FIBRE PLACEMENT

G. Sun[1*], R. Mitchell[2], Z. Chen[1], F. Omrani[3], M. Smith[3], J.P.A. Fairclough[1], and C. Pinna[1]

[1] Department of Mechanical Engineering, The University of Sheffield, Sheffield S1 3JD, UK,

[2] Sheffield Tomography Centre (STC), The University of Sheffield, UK, now at ZEISS Microscopy

[3] Advanced Manufacturing Research Centre, The University of Sheffield, Sheffield, UK

* Corresponding author (gsun8@sheffield.ac.uk)

Keywords: Tailored Fibre Placement (TFP), Carbon Fibre Reinforced Plastic composites, X-ray Computed Tomography, Mechanical Testing, Failure mechanisms

ABSTRACT

One of the promising automated fibre tow placement techniques for composite manufacturing is Tailored Fibre Placement (TFP) which provides flexibility for designing complex structures. The inherent anisotropic properties of carbon fibre reinforced plastic (CFRP) composites can be used during manufacturing through tailored placement of fibre tows to optimise lightweight and high performance simultaneously. In this study, the tensile response of a $[0/60/-60]_s$ TFP-manufactured CFRP composite was characterised through mechanical testing, carried out inside an X-ray microscope (XRM). Prior to loading a bespoke segmentation procedure was developed to clearly reveal the internal structure of the composite, including carbon fibre bundles and stitching threads. The sample was then progressively loaded with regular interruptions to scan the specimen and to characterise damage development. Results reveal the effect of stitching threads on both the morphology of carbon fibre bundles and the crack propagation process. The first crack initiated from the edge of the specimen and at mid-thickness. Further cracks appeared in the volume and in different plies as the load increased. A very fast propagation rate was recorded for these latter cracks which unloaded the first surface crack. This result emphasised the need for 3D observations to fully characterise the complex crack network eventually leading to failure of the specimen. Only a small amount of interlaminar delamination was observed, which was assumed to be prevented by the vertical stitching threads and no cracks were observed in the base material during the whole loading process.

1 INTRODUCTION

A primary characteristic of carbon fibre reinforced composites is their anisotropic properties with the maximum strength obtained along the reinforcement direction. Four advanced techniques, including Automated Tape Laying (ATL), Automated Tape Placement (ATP), Continuous Tow Steering, and Tailored Fibre Placement (TFP) techniques have been developed in the past decades for the manufacturing of variable stiffness composites to fully exploit the anisotropic properties of reinforcements. In comparison with the other three manufacturing processes, the TFP technique provides more flexibility in achieving complex fibre bundle trajectories [1].

The principle of the TFP technique is shown in Fig. 1 where fibre bundles are stitched onto a base material following a pre-defined placement path for the optimal design of composite structures. The orientation of continuous fibre tows can be changed by a rotational controller and in-plane movement of the base material along two perpendicular directions. Four main manufacturing parameters, namely the roving distance, the thread tension along with the stitch length and the stitch width due to a zigzag pattern, can be controlled during the manufacturing of TFP preforms.

Industrial applications of TFP-made composite structures are progressively increasing [e.g. 2 and 3] but the optimisation of this relatively new manufacturing technique requires a better understanding of the relationship between process parameters and mechanical properties of the material. 2D characterisations of TFP-made composites have been reported by Uhlig et al. [4] but are limited given the complex 3D geometry of the internal structure. Furthermore, although some studies have focused on the characterisation of the mechanical strength of TFP composites [5], the failure mechanisms under tensile loading are not well understood.

In this paper, the internal structure of a TFP-made CFRP composite is characterised in 3D using an X-ray Microscope (XRM) with the tensile response of the material characterised using in-situ mechanical testing inside the XRM. The microstructure of carbon fibre bundles and stitching threads are visualised through a bespoke segmentation approach. Damage mechanisms and crack development are then visualised in 3D for increasing applied loads.

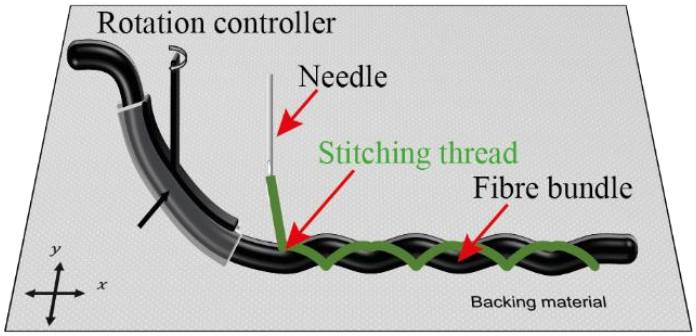

Figure 1: Principle of the TFP technique.

2 MATERIALS AND METHODS

Carbon fibre yarns, supplied by TORAY, were used for TFP manufacturing. The carbon fibre yarns were 800 tex, 12000 filament count with a density of 1.8 g/cm^3. The LY 564 epoxy resin and Aradur 2954 hardener were mixed as matrix material. A Serafil Comphil 180 polyester thread was used to stitch the fibre bundles onto the base material. An E-glass satin weave was used as the base material. A zigzag stitching pattern was selected during the manufacturing of the TFP preform. A $[0/60/-60]_s$ layer sequence for the TFP composite preform was prepared for consolidation using Resin Transfer Moulding (RTM).

The in-situ tensile test of the TFP-made CFRP composite was carried out using a 5kN Deben CT5000TEC loading stage inside a ZEISS Xradia 620 Versa X-ray Microscope (XRM) (see Fig. 2). A dog-bone shaped specimen was manufactured using waterjet cutting. Table 1 reports the six tensile loading steps designed to capture the crack propagation process up to failure. Gradually decreasing load increments were designed to capture crack propagation close to the failure point of the composite sample. A 4.15 × 3.88 mm^2 field of view (FOV) was selected with a voxel size of 4.36 μm^3 for the X-ray scans.

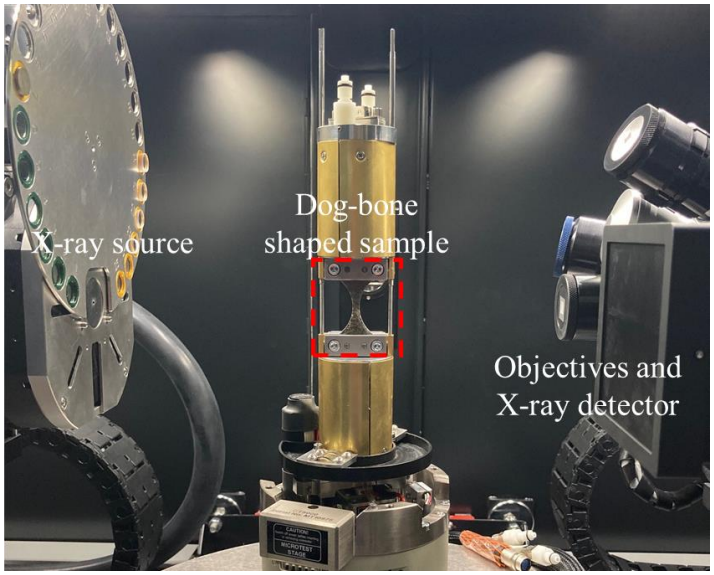

Figure 2: Dog-bone shaped sample loaded in the Deben CT5000TEC stage inside the XRM.

Steps	Load (N)	Load difference (N)
Step 0	0	-
Step 1	1240	1240
Step 2	2480	1240
Step 3	3720	1240
Step 4	4470	750
Step 5	4750	280

Table 1: X-ray scanning steps and corresponding tensile load values.

ORS Dragonfly software (version 2021.3) was used to process the reconstructed images for image segmentation, 3D visualisation, and quantitative analysis [6]. Due to the low contrast between carbon fibres and matrix and the high contrast produced by the glass fibres of the base material, the segmentation process could not be simply achieved by threshold-based segmentation methods. Several regions of interest (ROI) of the 3D image volume were extracted using the box-shaped extraction tool in ORS Dragonfly. The Anisotropic Diffusion (AD) filter was then used to separate the carbon fibre bundle phase from the matrix and stitching thread phases. A final manual segmentation operation was conducted for a more precise separation of the fibre bundles.

Since cracks appeared with low greyscale values in the 3D CT image volume, they could be easily identified in the region of interest by simply using a threshold-based segmentation approach. However, noise in the images caused during X-ray scanning was unavoidable. The amount of noise in CT results was assumed to be stable for each scan. As recommended by ORS Dragonfly, any voxel clusters segmented by a thresholding method with a number of voxels lower than nine were assumed to be noise and were removed by Region of Interest (ROI) refinement in ORS Dragonfly [6].

3 RESULTS AND DISCUSSIONS

The 3D segmented carbon fibre bundle structure (pink for layers 1 and 6, light blue for layers 2 and 5, light brown for layers 3 and 4), backing material (light grey) and stitching threads (dark blue) are shown in Fig. 3. The unsegmented parts were resin-rich areas created by the stitch tension from thread yarns. Different colours were used for representing different fibre directions.

Based on the segmented results, the morphology of each fibre bundle separated by stitching thread within the FOV was clearly presented. These stitching yarns were directly responsible for the fibre bundle waviness on the TFP preform. Triangular-shaped resin channels running from top to bottom were produced by vertical stitch threads, while smaller volumes of triangular prism resin channels were formed in the neighbourhood of horizontal stitch threads between two adjacent fibre bundles. It can be deduced that those channels somehow accelerate the resin injection velocity during RTM. Conversely, a highly compacted fibre bundle region slows the resin flow velocity. Lower interfacial properties between fibres and matrix are caused by a non-uniform resin flow speed.

Since the fibre bundles were pulled and stitched by stitch threads layer by layer, the thickness of each lamina was gradually decreased close to the base material as shown in Fig. 3. This was caused by the stitch tension during the TFP process to fix each fibre bundle at pre-designed positions for each layer. Layer 1 was stitched only once while layer 6 was compressed by upper layers several times. Such non-uniform thickness for each ply indicates that TFP-made composites cannot be treated as symmetric even if the presence of the base material is ignored. As shown in Fig. 3, the thickness of the bottom resin region is greater than that at the top, which can be explained through resin-rich zones and resin channels caused by stitch threads. The resin flowed much more easily into the base material region than into the carbon fibre bundles.

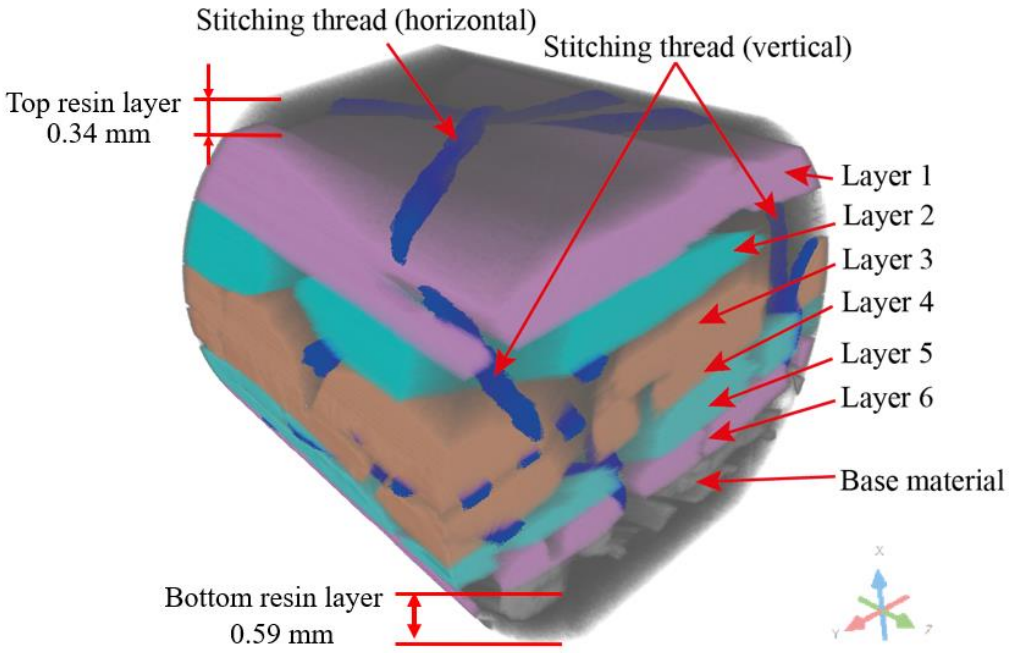

Figure 3: 3D segmentation and characterisation of the bundle structure in a TFP-made composite.

Cracks initiation and propagation were affected by fibre bundle features and the presence of the stitching thread. Fig. 4 shows crack initiation and propagation under different applied loads through the tensile test. 3D segmented cracks are shown in purple. The loading axis is horizontal in the images. The first transverse crack was initiated from the surface of the notched region of the dog-bone-shaped sample. This crack can be found in the -60° lamina located on layer 3 of the laminate (Fig. 4 (a)). While this initial crack slightly expands as the load increases, results show that further cracks initiate in the volume in plies 2 (60°), 3 (-60°), and 4 (-60°) (Fig. 4 (b)). These latter cracks grow much more extensively than the initial crack, progressively unloading it, with further cracks initiating as shown in Fig. 4 (c). This result, therefore, shows that surface observations would not be representative of the real damage process taking place in the TFP-made composite under tensile loading. Fig. 4 (d) demonstrates that the various cracks, which have developed in the volume coalesce, are forming a complex three-dimensional large crack network eventually leading to the failure of the specimen.

Matrix cracks could only be observed in layer 6, corresponding to the 0° fibre bundle orientation, when the tensile load reached 3720 N as shown in Fig. 4 (c), while no further transverse cracks were found in layer 1. This difference between layer 1 and layer 6 in terms of damage development was likely caused by the non-uniform load distributions due to the presence of the base material and non-equal thickness values of resin layers at both the top and bottom regions when loading.

Apart from transverse cracks in each ply, a small amount of interlaminar delamination can be observed for the later loading stages (see Fig. 4 (c) and (d)). This interlayer damage mode may have been prevented by the vertical stitching threads and therefore does not appear to be a dominant failure mode for TFP-made composites. This is unlike damage modes observed for more traditionally made unidirectional CFRPs under tension [7]. Furthermore, results showed no evidence of matrix cracking within the base material region.

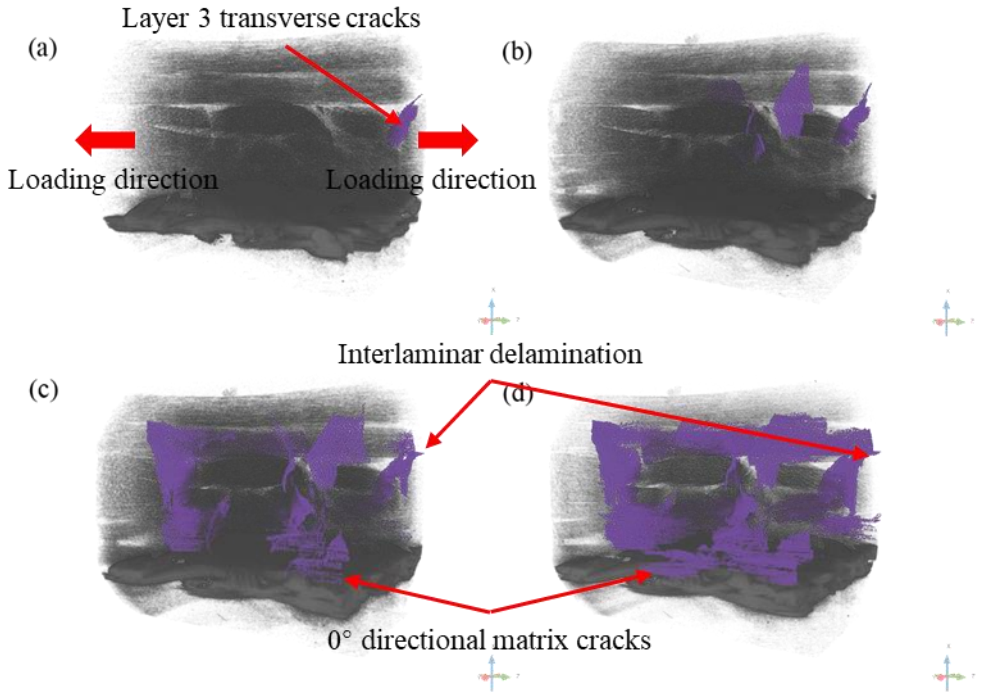

Figure 4: 3D segmented cracks (purple) and their propagation under loads of (a) 1240 N, (b) 2480 N, (c) 3720 N, and (d) 4750 N applied horizontally (z-direction) in the images.

Crack development has been quantified through the characterisation of crack volume and the ratio of increase in crack volume between loading steps. Crack volumes were counted using the number of voxels obtained following segmentation. The crack volume increase ratio was calculated based on the following equation:

$$R = \frac{V_{new} - V_{old}}{V_{old}} \times 100\% \quad (1)$$

where V_{new} represents the new accumulated number of voxels representing cracks and V_{old} the corresponding volume for the previous loading stage. Results are shown in Table 2. A very fast crack growth rate can be found up to 3720 N with a more than 2200% increase in crack volume between load stage 1 and load stage 3 while a much lower crack growth rate is observed for the final loading stages approaching the failure point. It is assumed that the low interfacial properties between fibres and resin is the reason for the huge amount of transverse cracks observed during the loading stages from 1240 N to 3720 N.

Load (N)	Crack volume (voxels)	Crack volume increase (%)
1240	78, 100	-
2480	520, 472	566.4%
3720	1, 804, 051	246.6%
4470	1, 978, 993	9.6%
4750	2, 653, 305	34.1%

Table 2: Evolution of crack volume and increase in crack volume ratio with applied load.

4 CONCLUSIONS

This study has shown for the first time a 3D visualisation of the microstructure of TFP-made composites using micro X-ray Computed Tomography and a characterisation of the evolution of damage mechanisms operating in the complex microstructure of the composite under tensile loading through in-situ mechanical testing.

Results revealed the influence of stitching threads on the formation of resin-rich regions and the non-uniform thickness of layers in the laminate during the manufacturing process. Cracks under tensile loading were initiated from the surface of the specimen in the -60° lamina. Further cracks initiated in the volume in plies 2 (60°), 3 (-60°), and 4 (-60°), as the load increased and showed a much faster propagation rate compared to the initial crack which became progressively unloaded. As the load further increased multiple cracks progressively coalesced into a complex 3D network eventually leading to the failure of the specimen. Interlaminar delamination was barely observed during the test suggesting a direct effect of the vertical stitching delaying delamination. This study has therefore shown the need to characterise TFP-made composites in 3D to fully understand the influence of their complex microstructure on the failure process in order to optimise the manufacturing process.

ACKNOWLEDGEMENTS

Authors acknowledge the University of Sheffield X-ray CT Facility funding from EPSRC (EP/T006390/1).

REFERENCES

[1] P. Mattheij, K. Gliesche, and D.Feltin “Tailored Fiber Placement – Mechanical properties and applications”. *J.Reinf. Plast. Compos.*, vol. 17, no. 9, 1998.

[2] Richter, E., Spickenheuer, A., Bittrich, L., Uhlig, K. and Heinrich, G., 2015. Applications of variable-axial fibre designs in lightweight fibre reinforced polymers. In *Materials Science Forum* (Vol. 825, pp. 757-762). Trans Tech Publications Ltd.

[3] Uhlig, K., Spickenheuer, A., Bittrich, L. and Heinrich, G., 2013. Development of a highly stressed bladed rotor made of a cfrp using the tailored fiber placement technology. *Mechanics of Composite Materials*, *49*, pp.201-210.

[4] Uhlig, K., Tosch, M., Bittrich, L., Leipprand, A., Dey, S., Spickenheuer, A. and Heinrich, G., 2016. Meso-scaled finite element analysis of fiber reinforced plastics made by Tailored Fiber Placement. *Composite Structures*, *143*, pp.53-62.

[5] Uhlig, K., Spickenheuer, A., Gliesche, K. and Karb, I., 2010. Strength of CFRP open hole laminates made from NCF, TFP and braided preforms under cyclic tensile loading. *Plastics, rubber and composites*, *39*(6), pp.247-255.

[6] Dragonfly 2021.3 [Computer software]. Object Research Systems (ORS) Inc, Montreal, Canada, 2020; software available at http://www.theobjects.com/dragonfly.

[7] Wisnom, M.R., 2012. The role of delamination in failure of fibre-reinforced composites. *Philosophical Transactions of the Royal Society A: Mathematical, Physical and Engineering Sciences*, 370(1965), pp.1850-1870.